Elliptical galaxies

Questions
- are bulges of spirals similar to ellipticals?
- what causes the flattening – rotation or something more complex?
- what is the true distribution of shapes of E galaxies?
  – are some triaxial?
- can we model stellar dynamics and luminosity distribution self-consistently?

Luminosity distributions

ref: Mihalas & Binney + Binney & Merrifield

Many but not all ellipticals can be fit by a de Vaucouleurs "$r^{1/4}$" law

$$\log \frac{I(r)}{I(r_e)} = -3.33\left[\left(\frac{r}{r_e}\right)^{1/4} - 1\right]$$

r_e is 'effective radius' – contains 50% of luminosity

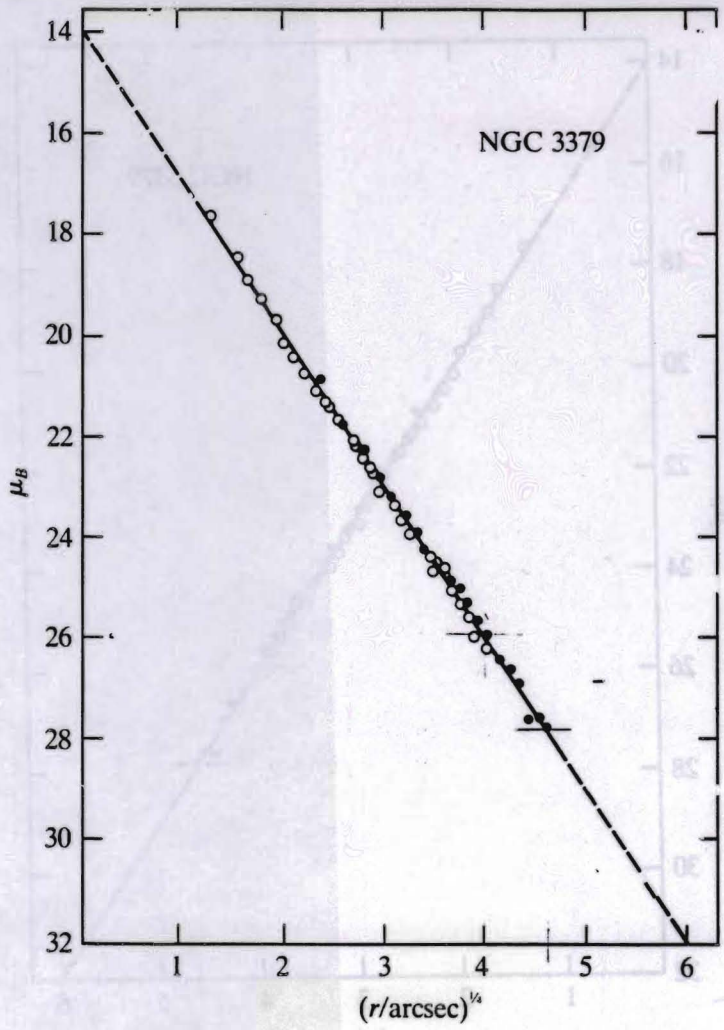

Figure 5-12. The brightness profile of the giant E1 galaxy NGC 3379. The dots and circles are photoelectric measurements by different observers along the galaxy's east-west profile. Note the beautiful fit to the $r^{1/4}$ law (see text) over 10 mag of surface brightness. [From (.)6), by permission. Copyright © 1979 by the Am.ican Astronomical Society.]

different values of r_c give different central concentrations

(note that data often looks better on a log-log plot!)

Empirical description only ..... although various n-body models can reproduce $r^{1/4}$ laws .....

Sersic profiles: a more general equation that includes $R^{1/4}$ and exp functions as special cases.

$$I(r) = I_0 \exp\left(-\left(\frac{r}{r_0}\right)^{1/n}\right)$$

In magnitudes, $$\mu(r) = \mu_0 + 2.5 \log_e\left[\exp\left(\frac{r}{r_0}\right)^{1/n}\right]$$

Q What values of n reduce to an exponential (disk) profile ?

an $R^{1/4}$ profile ?

$n = 4 \Rightarrow R^{1/4}$

$n = 1 \Rightarrow$ exponential

Problem

List some of the possible difficulties in obtaining an accurate brightness profile of a galaxy. Will the faint bits or the bright bits be easier ?

Photometric properties and structure

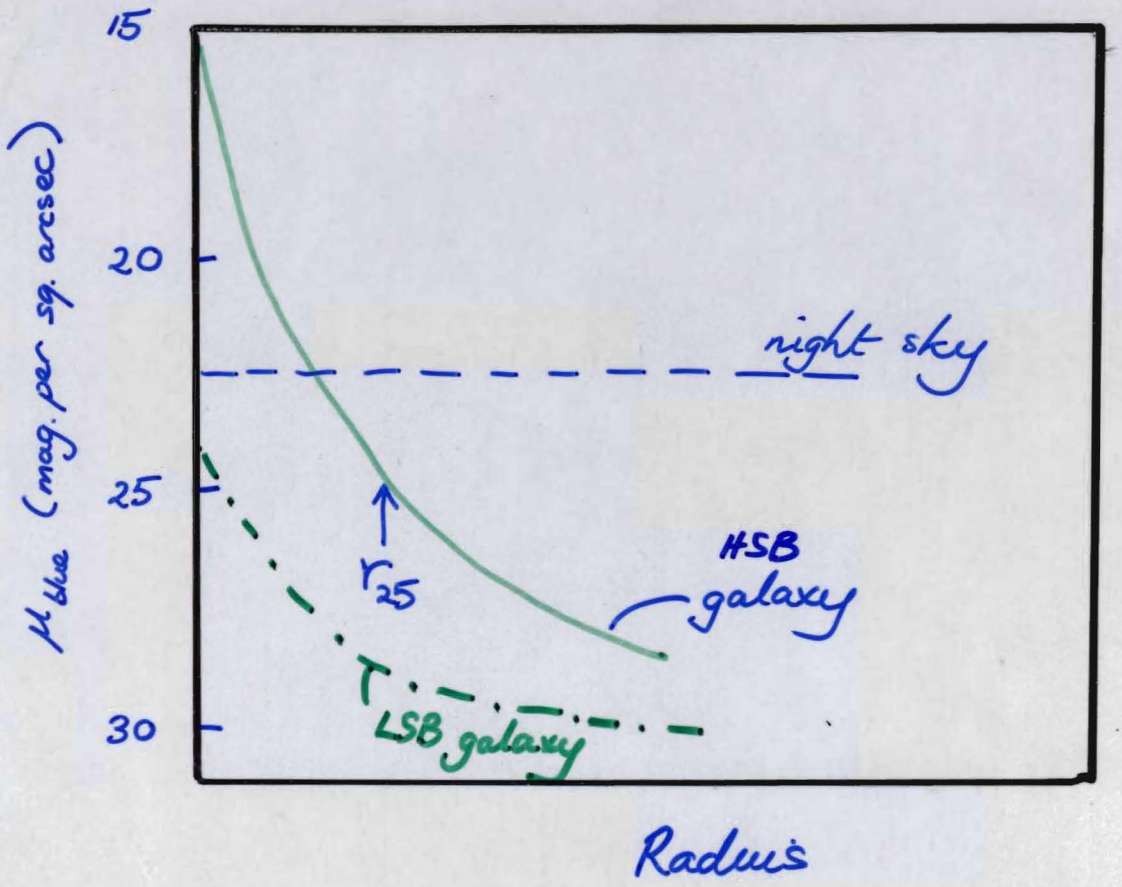

Observations in 90's : CCD imagers (optical λ)
IR arrays ($1-5\mu$)

Only the brightest portion of most galaxies is brighter than night sky.

Isophotal radius : apparent diameters on Palomar sky survey plates correspond to an isophote of ~25 B mag/sq arcsec.

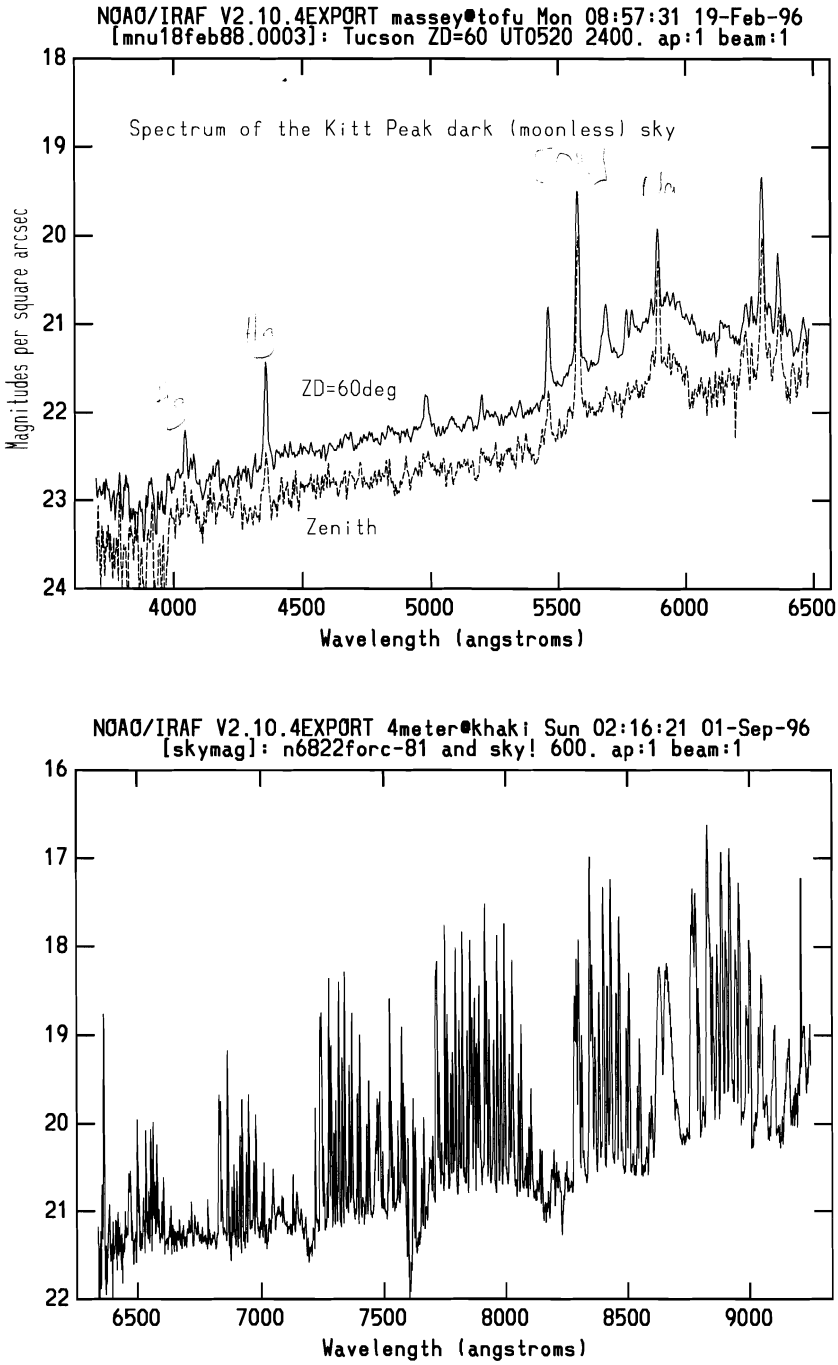

Figure 9: The spectrum of the moonless Kitt Peak sky. In the "optical" region ($\lambda\lambda 4000 - 6500$) the continuum rises from 23 mag/arcsec^2 to 21.5, with the major artifical source the NaD lines from street-lights (see Massey, Gronwall & Pilachowski 1990 PASP, 102, 1046). Further in the red, the sky spectrum is dominated by OH emission lines.

King models

These models have a theoretical (dynamical) basis : combination of light distribution from an isothermal sphere with a tidal truncation at large radii.

Distribution function in stellar dynamics — describes the 'phase space density' of the system

$$f(\underline{x}, \underline{v}, t)\, d^3\underline{x}\, d^3\underline{v}$$

number of stars in the small volume $d^3\underline{x}$ centered on $\underline{x}$, with velocities in the small range $d^3\underline{v}$ centered on $\underline{v}$.

In $\equiv^m$, this is not a function of t

In simple spherical case, it is possible that $f = f(E)$ only

E = total energy.

Isothermal sphere

$$f_I(E) = (2\pi\sigma^2)^{-3/2} \rho(0) \exp\left(\frac{\Phi(0) - E}{\sigma^2}\right)$$

ρ is density

$\Phi(0)$ is potential energy @ center of system

E is total energy

For large radii $\rho \propto \frac{1}{r^2}$

..... infinite mass, unfortunately (why?)

King truncates distribution function @ large radii:

take some maximum allowed energy E_t

$$f_k(E) = 0 \qquad E \geq E_t$$

$$= f_I(E) - f_I(E_t) \qquad E < E_t$$

$$= (2\pi\sigma^2)^{-3/2} \rho_1 \left[\exp\left(\frac{E_t - E}{\sigma^2}\right) - 1\right]$$

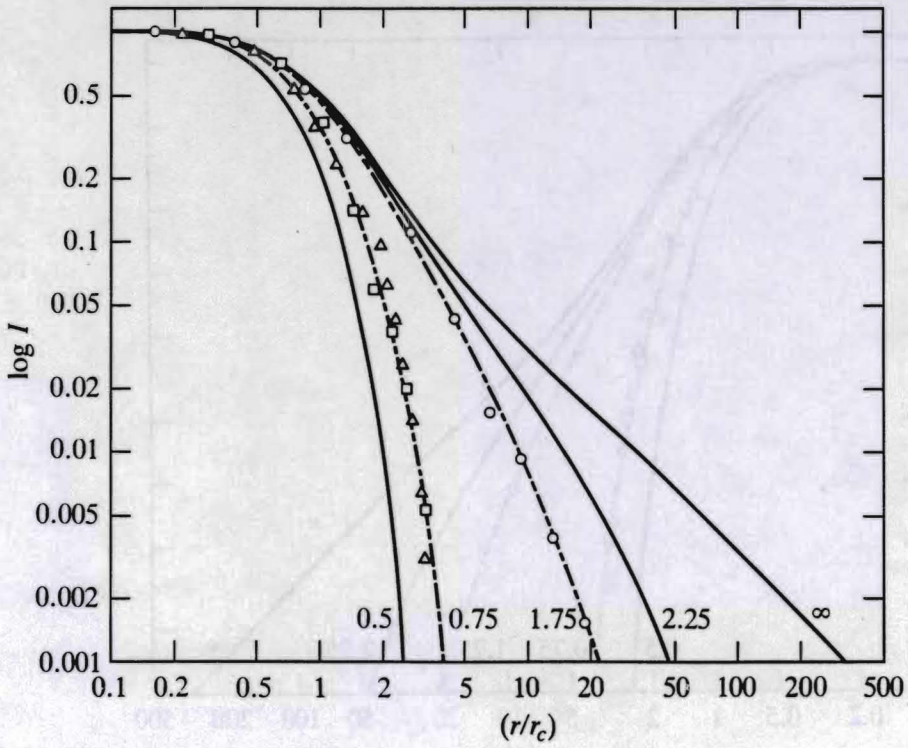

Figure 5-9. Star-density profiles of globular clusters and dwarf ellipticals. The data points are for the Sculptor dwarf galaxy (△), the globular cluster NGC 5053 (□), and the globular cluster NGC 6388 (○). The curves are members of King's family of theoretical profiles and are labeled by their c values [$c = \log(r_t/r_c)$]. The sets of data points have been shifted vertically and horizontally until their best-fitting King curves have $r_c = 1$. [From data published in **(H1)**, **(I1)**, **(K1)**.]

globular clusters ($\sim 10^5 M_\odot$) and some dwarf (dSph's) ellipticals ..... simpler systems ..... are often well fit by King models

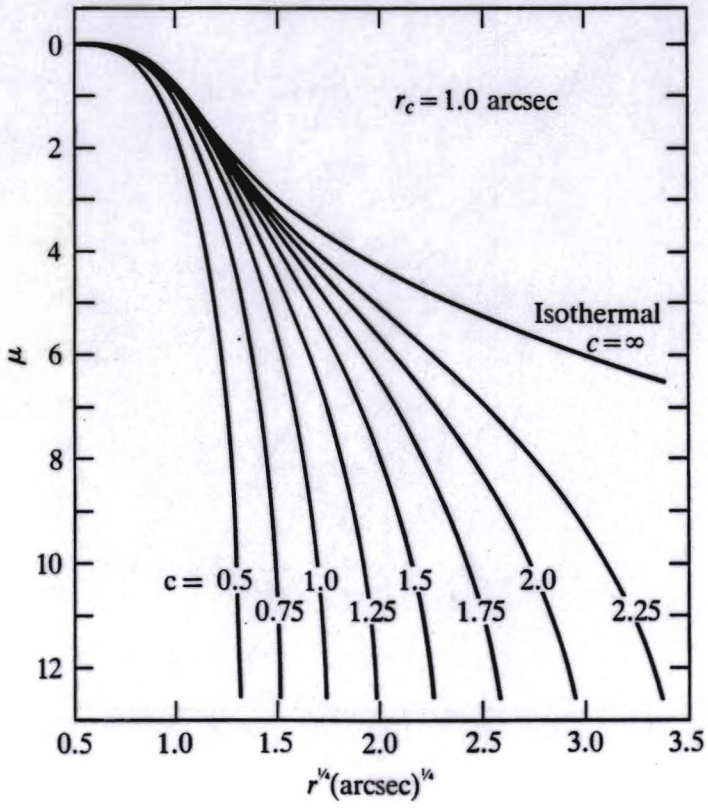

Mihalas & Binney

Figure 5-13. King model brightness profiles plotted on scales for which the de Vaucouleurs law is a straight line. Giant ellipticals are generally best fit by curves having $2 < c < 2.35$. [From **(K4)**, by permission. Copyright © 1977 by the American Astronomical Society.]

Parameterized by variables:

core radius r_c : $I(r_c) = \frac{1}{2} I(0)$

Tidal radius r_t $I(r_t) = 0$

concentration $c = \log\left(\frac{r_t}{r_c}\right)$

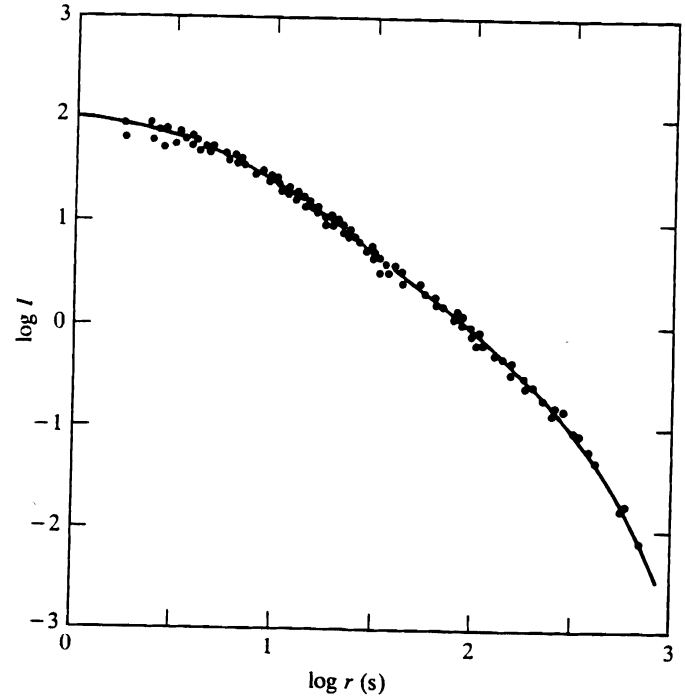

Figure 5-11. The brightness profile of NGC 4472 (data points) is well fitted by the $c = 2.35$ King profile (curve). It follows from this and Figure 5-13 that these observations of NGC 4472 cannot be so well fitted with the de Vaucouleurs law. [From (**K2**), by permission. Copyright © 1978 by the American Astronomical Society.]

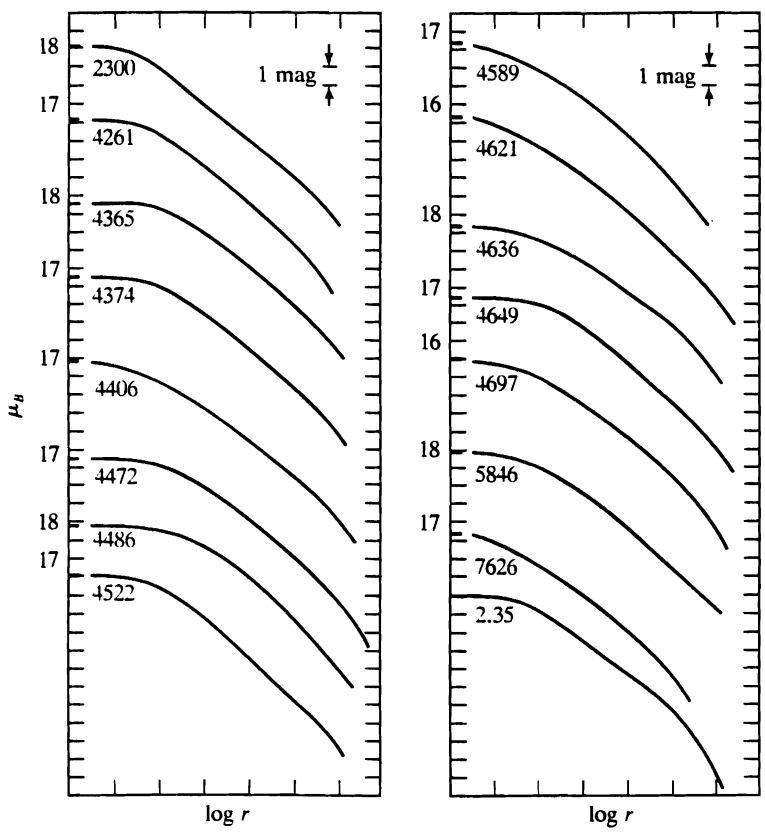

Figure 5-10. Brightness profiles of 15 elliptical galaxies, labeled by their NGC numbers, as measured by King. The curve labeled 2.35 is one of King's theoretical curves with $c = 2.35$. [From (**K2**), by permission. Copyright © 1978 by the American Astronomical Society.]

Velocity ellipsoid and galaxy shape

Q There are two different things that determine the shape of an elliptical galaxy, one related to mean orbital velocity of stars, one to the dispersion in their velocities. What might they be?

→ rotational flattening

→ anisotropic velocity dispersions

lower-luminosity ellipticals (& galaxy bulges) are flattened with rotation.

High-luminosity ellipticals have no mean rotation, only anisotropic velocity dispersions

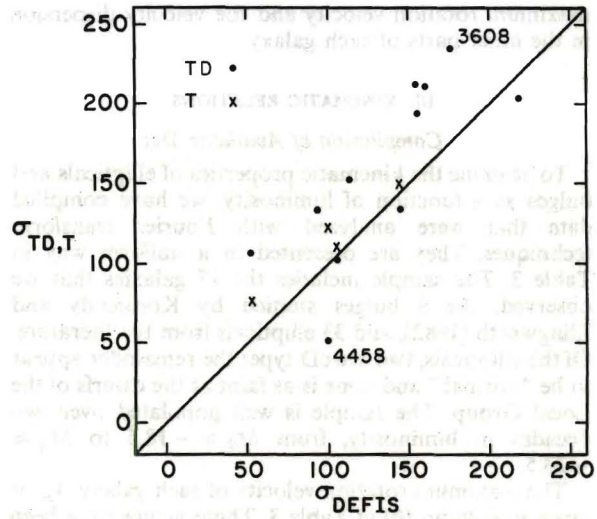

FIG. 2.—Velocity dispersions from this paper plotted against those of Tonry and Davis (1981*a*, *b*) and Tonry (1981).

may be influenced by the presence of a central mass concentration or velocity anisotropy, and we therefore consider $\bar{\sigma}$ to be a more representative dispersion. As expected, $\bar{\sigma}$ is usually smaller than σ_0, but only in a few cases does the difference exceed 20%.

Estimates of the effective radii, r_e, for the ellipticals are given in arc seconds in column (5) of Table 3. The values of the r_e for the majority of galaxies in the sample were calculated from the effective diameters, A_e, in the RC2, which were determined from multiaperture photoelectric photometry or detailed photographic photometry. For seven galaxies, A_e was not given, and so we have taken $r_e = \frac{1}{6}D_{25}$, where D_{25} is the diameter at the $B = 25$ mag arcsec^{-2} isophote. A comparison of the two estimates of the r_e for the majority of galaxies in our sample shows that this procedure leads to no systematic bias and an rms scatter of only 17%.

For comparison with theoretical models, it is preferable to have measurements of ellipticity and kinematics in the same part of a galaxy. Ellipticities at the appropriate radii are available for only 16 of the galaxies in our sample from the studies of King (1978) and Leach (1981). We have compared their ellipticities at r_e with those at $\frac{1}{2}D_{25}$ ($\sim 3r_e$) from the RC2 and find no systematic difference. Except when noted, the ellipticities given in column (4) of Table 3 are those from the RC2 or are averages of the RC2 values and the Leach and King values at r_e. In individual cases, these estimates may not reflect the ellipticity in the central regions of a galaxy, but they should be appropriate for the sample as a whole.

To estimate absolute magnitudes, we have assigned the galaxies to groups and have used the mean velocity of each group as a distance indicator. The name of the group and the adopted group velocity are given in columns (2) and (3) of Table 3. Group membership was determined from de Vaucouleurs (1975), from our inspection of the Palomar and ESO sky surveys, and from recession velocities in the lists of Tonry and Davis (1981*a*,*b*), Rood (1981), Sandage and Visvanathan (1978), Sandage (1978), and the RC2. Apparent magnitudes, on the B_T system, were taken from the RC2. One set of absolute magnitudes, M_B^{UH}, given in column (10) of Table 3, was derived assuming a uniform Hubble flow with $H_0 = 50$ km s^{-1} Mpc^{-1}. Another set of magnitudes, M_B^{VF}, given in column (11), was derived using a model of the Virgocentric flow, equation (2) in Schechter (1980) with $\gamma = 2$, and an infall velocity of 300 km s^{-1}. The distance modulus and center of the Virgo Cluster were taken to be 30.98 (Mould, Aaronson, and Huchra 1980) and $\alpha(1950) = 12^h27^m.6$, $\delta(1950) = 12°56'$. In this case, the far-field Hubble constant is $H_0 = 84$ km s^{-1} Mpc^{-1}. Entries marked with plus signs have triple-valued distances on the inflow model, and only the intermediate solutions are tabulated. An extinction correction of 0.13 ($\csc|b| - 1$) and a K-correction of $5.32z$ have been applied to both sets of magnitudes.

b) *Relation between Rotation and Luminosity*

In Figure 3 we have plotted $V_m/\bar{\sigma}$ against ellipticity. The filled circles show ellipticals fainter than $M_B^{UH} = -20.5$ and the open circles show the brighter galaxies. It is clear that the faint ellipticals rotate more rapidly than most of the bright ellipticals. Also shown in this diagram is the relationship derived from the tensor virial theorem under the assumption that ellipticals are oblate spheroids of constant ellipticity with isotropic velocity distributions (Binney 1978). The predicted ratio, $(V/\sigma)_{OI}$, follows if the rotation curve and dispersion profile are

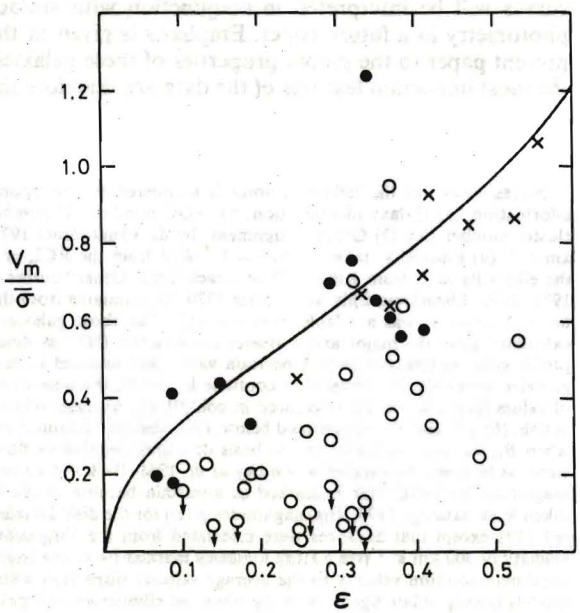

FIG. 3.—The quantity $V_m/\bar{\sigma}$ against ellipticity. Ellipticals with $M_B^{UH} > -20.5$ are shown as filled circles; ellipticals with $M_B^{UH} < -20.5$, as open circles; and the bulges of disk galaxies, as crosses. The solid line shows the $(V/\sigma, \epsilon)$-relation for oblate galaxies with isotropic velocity dispersions (Binney 1978).